BMC Oral Health

RESEARCH

Open Access

Biomechanical evaluation of six zygomatic implants versus four zygomatic implants combined with dental implants in the treatment of different maxillary defects

Zeynep Gümrükçü[1*], Emre Balaban[1] and Zeynep Bayramoğlu[2]

Abstract

Background This study aims to compare the biomechanics of six zygomatic implants (ZIs) and dental implants (DIs) combined with four ZIs with different maxilla defects.

Methods Three-dimensional constructs of the ZIs, DIs human skulls, and maxillary prostheses were created using SolidWorks Software (Version 2015, Dassault Systems SolidWorks Corporation, Waltham, MA, USA). Eight finite element models of the skull with four different alveolar defect types (0–4) were constructed. Type 0: No defect; Type 1: Bilateral posterior defects; Type 2: Right posterior defect; Type 3: Anterior and left posterior defects; Type 4: Bilateral posterior and anterior defects. In two models with the same defect type (for defect types 0–2), six ZIs or two DIs combined with four ZIs were inserted into the maxilla. Six ZIs were inserted in the maxilla models with defect types 3 and 4. Vertical (150 N) and masseteric (300 N) loads were simulated on the prosthesis. The maximum Von Mises stress in the implants/surrounding bone and bone deformation were evaluated.

Results The maximum Von Mises stresses in bone/implant were found highest in the defect type 2 model with four ZIs combined with two DIs. The lowest maximum Von Mises stress for bone was detected in the model with defect type 0 and with six ZIs.

Conclusion Among the four types of defects, the posterior unilateral defect caused the highest stress value.

Keywords Zygomatic implant, Alveolar defect, Six zygomatic implants, Quad zygomatic implant, Finite element analysis

*Correspondence:
Zeynep Gümrükçü
zeynep_dt@hotmail.com
[1]Department of Oral and Maxillofacial Surgery, Faculty of Dentistry, Recep Tayyip Erdoğan University, Rize, Turkey
[2]Department of Oral and Maxillofacial Surgery, Faculty of Dentistry, Atatürk University, Erzurum, Turkey

Background

Tooth loss is usually a condition that can result from advanced tooth decay, periodontal disease, trauma, malign pathology, infection and other causes [1]. Maxillary edentulism cases have become an increasing problem worldwide and a serious threat to patient daily comfort. For the maxilla, especially after resection due to malignant tumor formations, restoring the lost aesthetics and function is quite problematic. Especially patients who have undergone oncological resection experience serious problems in terms of speaking, chewing, swallowing and quality of life. In such cases, nonvascular flaps, local flaps, microvascular free flaps, bone grafts applied with titanium plates or screws, conventional prosthetic obturator application or zygomatic/dental implant-supported obturator prosthesis application can be counted among the treatment alternatives used to restore the lost of oral function and aesthetics [2]. Various augmentation/grafting procedures needed to increase the amount of bone before implant placement and to make implant placement possible. However, augmentation procedures are a laborious process whose results are not always predictable and require additional surgery for the patient. For this reason, techniques that enable implant placement without the need for augmentation have recently been developed and tested [3].

Zygoma implants (ZIs) are the treatment option for patients who are not suitable for conventional dental implant (DI) placement, who have severe maxillary alveolar bone resorption, or who have partial or complete defects in the maxillary bone as a result of oncological resection. Conventional ZI rehabilitation has been applied as one of the popular treatments to provide support for a fixed and removable prosthesis in conjunction with/without DIs for atrophic or defected maxilla [3, 4]. ZIs are known as extremely advantageous treatments due to their high success rates, which can restore the lost functional and aesthetic features and support prosthesis as an alternative to the grafting protocol [5, 6]. The standard technique was described in 1988 by Branemark [7]. Branemark suggested two ZIs at the posterior region and 2 to 4 DIs in the anterior region in the standard technique. The ZI inserts the alveolar bone at the location of the second premolar teeth location, from the top of the crest, passes through the maxillary sinus, and is placed into the zygomatic bone [8].

ZIs are often used in combination with anterior DIs. However, in some cases, it is impossible to insert anterior DIs due to the atrophy of bone loss (especially after malignity resections), as described in the standard technique. In the literature, to provide solutions to these conditions, quad ZIs were applied without an anterior DI [6, 9, 10]. In literature, it has been indicated that one to three implants can be used for the ZI [7] The use of multiple ZIs in the rehabilitation of defected maxilla has been reported to be a safe technique and a good alternative to bone augmentation procedures [11]. The use of 3 ZIs on each side of the maxilla to support a dental prosthesis has been previously described in the literature [12].

Although there are many studies focused on double and quad ZIs with/without anterior DI in the literature, there is no study addressing the comparison of the six zygomatic approaches with quad approaches. This study aims to provide preliminary biomechanical information for clinical studies by comparing quadruple and six-fold ZI applications.

Methods

The study was carried out by the Faculty of Dentistry, in the Oral and Maxillofacial Surgery Department at Recep Tayyip Erdogan University in 2020.

Modelling of the skull

A three-dimensional (3D) finite element solid model of a human skull was constructed with the help of a scanning device (Metris Nikon, Metris MCA 30, Nikon, 2009 Italy). SolidWorks Computer-Aided Design program (Version 2015, Dassault Systems SolidWorks Corporation, Waltham, MA, USA) in the initial graphics exchange specification format was used to construct the solid model of the human skull anatomical morphology. The maxilla was modeled to include cancellous bone surrounded by 1.5 mm of cortical bone to represent bone type D2 for the anterior maxilla and surrounded by 0,75 mm of cortical bone to represent bone type D3 for the posterior maxilla according to Lecholm and Zarb classification [13]. The contact between cortical bone and cancellous bone was assumed to be 'Bond type'. The created model was transferred to the ANSYS Workbench 12.01 (ANSYS Inc.).

The maxilla was separated into three segments;

1. **PS_R- Right posterior segment**: The right posterior segments (the segment between the right tuber maxilla and right first premolar tooth).
2. **PS_L: Left posterior segment**: The left posterior segments (the segment between the left tuber maxilla and left first premolar tooth).
3. **AS: Anterior segment)**: The anterior segment (the segment between two canine teeth).

Five types of maxillary defect were constructed;

1. **Defect Type 0**: Maxilla kept intact, no alveolar defect was simulated on models.
2. **Defect Type 1**: The alveolar defect was simulated on the PS_R and PS_L segments.

3. **Defect Type 2**: The alveolar defect was simulated only on the PS_R segment.
4. **Defect Type 3**: The alveolar defect was simulated on the AS and PS_L segments.
5. **Defect Type 4**: The alveolar defect was simulated on the AS, PS_R and PS_L segments.

With regard to the defect types and implant planning, eight treatment scenarios were simulated on models. All scenarios are summarized in Table 1; Fig. 1. The eight planned scenarios are described below;

Scenario 1 Defect type 0 was simulated on the models. Two ZIs were placed into the maxilla model at the location of the first premolar and second premolar teeth bilaterally, and DIs were placed on the maxilla bilaterally at the location of lateral incisors (Fig. 1a).

Scenario 2 Defect type 0 was simulated on the models. Three ZIs were placed in the maxilla model at the location of the first premolar, second premolar, and first molar teeth bilaterally (Fig. 1b).

Scenario 3 Defect type 1 was simulated on the models. Two ZIs were placed on the maxilla model at the location of the first premolar and second premolar teeth bilaterally, and DIs were placed on the maxilla bilaterally at the location of lateral incisors (Fig. 1c).

Scenario 4 Defect type 1 was simulated on the models. Three ZIs were placed at the location of the first premolar, second premolar, and first molar teeth bilaterally (Fig. 1d).

Scenario 5 Defect type 2 was simulated on the models. Two ZIs were placed at the location of the first premolar and second premolar teeth bilaterally, and Dis were placed on maxilla bilaterally at the location of lateral incisors (Fig. 1e).

Scenario 6 Defect type 2 was simulated on the models. Three ZIs were placed at the location of the first premolar, second premolar, and first molar teeth bilaterally (Fig. 1f).

Scenario 7 Defect type 3 was simulated on the models. Three ZIs were placed at the location of the first premolar, second premolar, and first molar teeth bilaterally (Fig. 1g).

Scenario 8 Defect type 4 was simulated on the models. Three ZIs were placed at the location of the first premolar, second premolar, and first molar teeth bilaterally (Fig. 1h).

Defects were created by trimming the alveolar crest using the 'cut' command on the program, and approximately 1.5–2 cm in height alveolar crest was removed from the model following the predetermined scenarios.

Modelling Implants

ZI and DIs were modeled by SolidWorks software by referring to the surface morphology and dimensions of the Nobel Biocare Implant System. Six 48-mm ZIs (46, 48, and 50 mm, Nobel Biocare AB) with an abutment 5 mm in height and two regular DIs (3.75–13.0 mm, Nobel Biocare AB) with abutments 5 mm in height. The length of the ZI was determined by measuring the distance between the maxillary alveolar crest and the jugal point of the zygomatic bone [14]. After the implants were modelled, they were mounted in their planned locations in 8 different scenarios in the modeled skull model. It was also assumed that the skull models and implants were in full contact (assuming exact osseointegration).

The hybrid prosthesis was modeled as a superstructure (Fig. 2). Boundary conditions on the model used in the study were applied to generate force-displacement results by restraining movement in the X, Y and Z directions. of the model [15, 16]. Relevant material properties were assigned to each planned texture/structure. All materials for FEA models were assumed to be isotropic, homogenous, and linearly elastic [9]. The material properties of all models are shown in Table 2.

Eight models of all predetermined scenarios were transferred to the ANSYS Workbench program to

Table 1 Summary of eight models

Model	Defect Type	Implant Number		Implant Location Zygomatic/Dental		Number of element	Number of Nodes
		Zygomatic	Dental	Right	Left		
S1-4Z2D	0	4	2	5 – 4/2	5 – 4/2	711,825	1,284,639
S2-6Z	0	6	0	6-5-4	6-5-4	698,329	1,105,971
S3-4Z2D	1	4	2	5 – 4/2	5 – 4/2	567,287	919,227
S4-6Z	1	6	0	6-5-4	6-5-4	533,987	902,713
S5-4Z2D	2	4	2	5 – 4/2	5 – 4/2	665,308	1,016,432
S6-6Z	2	6	0	6-5-4	6-5-4	658,726	1,023,198
S7-6Z	3	6	0	6-5-4	6-5-4	545,329	911,457
S8-6Z	4	6	0	6-5-4	6-5-4	479,548	783,568

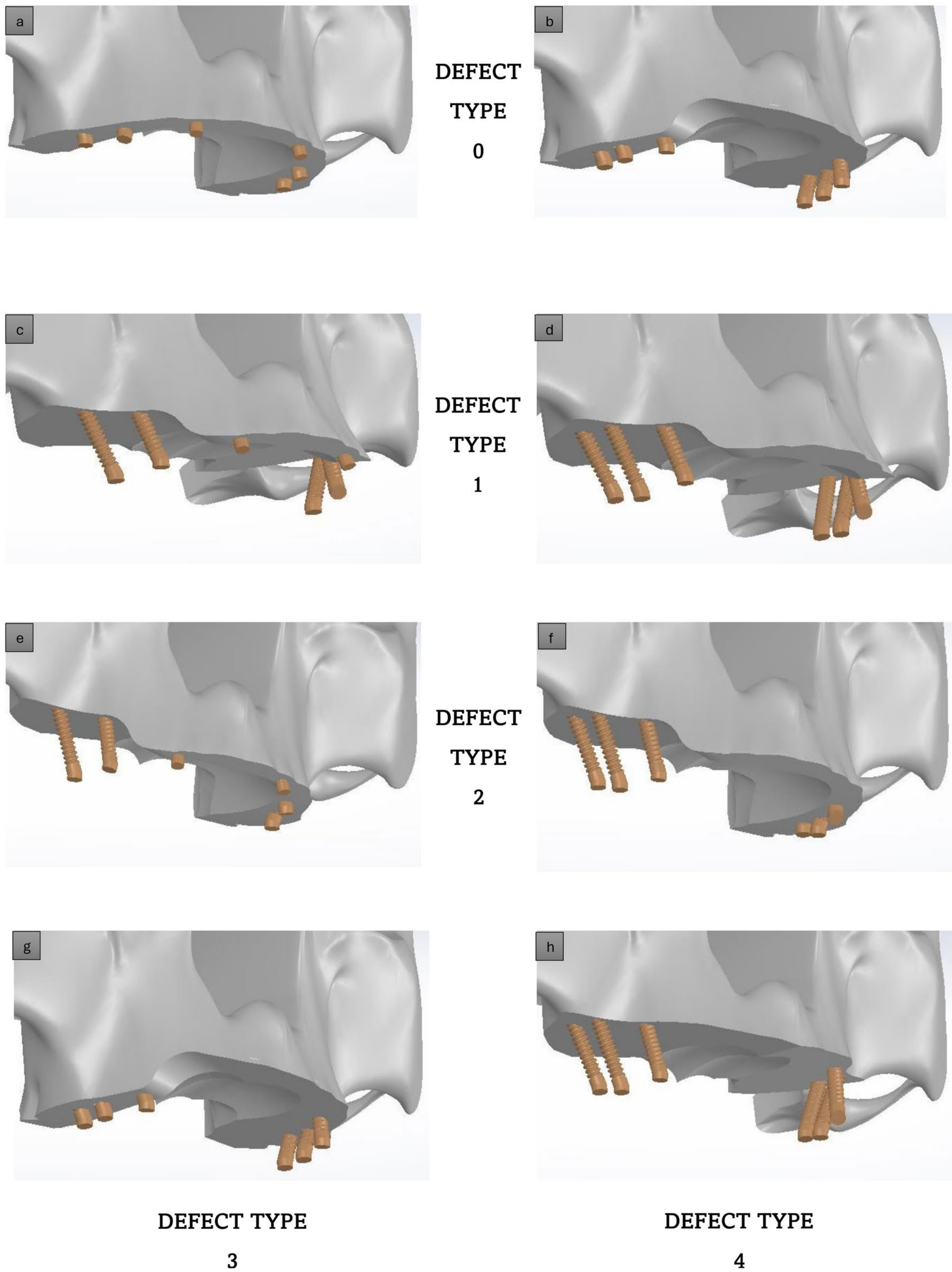

Fig. 1 Eight implant scenarios; **a**: Scenario 1, **b**: Scenario 2, **c**: Scenario 3, **d**: Scenario 4, **e**: Scenario 5, **f**: Scenario 6, **g**: Scenario 7, **h**: Scenario 8

generate the FEA models. In our study, "convergence analysis" was performed to determine the ideal element size and an element size of 0.8 mm was used as the meshing requirement for all FEA models.

Modelling bar attachment and prosthesis

The cortical and trabecular bone, implants with multi-unit abutments, bar attachment in rectangular form. The bar attachment was modeled in a rectangular form. This

Fig. 2 Assembly of the modeled parts

Table 2 Mechanical properties of materials used in the 3D finite models

Material	Elastic Modulus (E) (MPa)	Poisson Ratio (v)
Acyrilik	3,000	0.35
Cortical Bone	13,700	0.30
Cancellous Bone	1,370	0.30
İmplant (Titanium)	103,400	0.35
Bar (Chromium-Nickel)	200,000	0.33

was 2 mm in width and was placed 1.6–2 mm above the crestal bone. The material properties of a chromium-nickel (Cr-Ni) alloy were assigned to the bar attachment. The bar attachment and implant were assumed to be in a merged connection. Hybrid prosthesis were modeled and assembly of units were done (Fig. 2).

Loading Conditions

Vertical force (150 N) was applied to the contact points of the first premolar, second premolar, and first molar teeth.[9, 17] A simulated masseter load of 300 N with force components of 12.42 N on the x-axis, 53.04 N on the y-axis, and 25.14 N on the z-axis was applied to the insertion area of the masseter muscle on the zygomatic arch and zygomatic process of the maxilla on the left and right side of the bone [14, 15].

Von Mises stress is typically used in materials that are ductile or yield before breaking. This is because it takes into account the shear stresses that can cause yielding. Principle stress is used in brittle materials, such as ceramics, which do not yield before breaking. Maximum principal stresses describe the stress concentrated in a particular region. On the other hand, von Mises stress is a scalar measurement obtained from the stresses acting on any structure. Since bone is a ductile structure and therefore the forces acting on the implant can be distributed to the surrounding distant tissues, it was deemed appropriate to use von Mises stress in this study to make a scalar measurement [16].

The maximum Von Mises stress (MPa), in and around the implant and bone deformation values (mm), were evaluated in each model, and the results were visualized using color distribution scales.

Results

The maximum Von Mises stress values, found in the surrounding bone, are listed in Table 3. The maximum Von Mises stress value was found in the model S5-4Z2D as 84.257 MPa. The stress distributions are shown in Fig. 3. This value was followed by S6 with 79.365 MPa, S7 with 79.302 MPa, S3 with 74.867 MPa, S8 with 73.039 MPa, S4 with 73.025 MPa, S1 with 65.054 MPa and S2 with 61.25 MPa (The maximum Von Mises stress values were ranked as S5 > S6 > S7 > S3 > S8 > S4 > S1 > S2). The lowest Von Mises stress value (61.25 MPa) was found in the S2-6Z model (Fig. 3).

The maximum Von Mises stresses, seen in the implants, are shown in Table 3. The highest stress was seen in the model S5-4Z2D (138.33 MPa). This value was followed by S7 with 135.02 MPa, S6 with 134.51 MPa, S1 with 114.07 MPa, S8 with 107.347 MPa, S4 with 107.293 MPa, S3 with 102.884 MPa and S2 with 96.544 MPa (The maximum Von Mises stresses were ranked as S5 > S7 > S6 > S1 > S8 > S4 > S3 > S2). The maximum von Mises stress values

Table 3 Maximum Von Mises Stress in bone, implants and bone deformation

Models	Maximum Von Mises Stress (MPa)				Bone Deformation (mm)	
	Surrounding Bone		Zygomatic Implant		V	L
	V	L	V	L		
S1-4Z2D	65.054	5	114.07	5 (Bilaterally)	0.0175	5 (Bilaterally)
S2-6Z	61.25	6	96.544	6 (Bilaterally)	0.0088	5 (Bilaterally)
S3-4Z2D	74.967	5	102.884	5 (Bilaterally)	0.0302	5 (Bilaterally)
S4-6Z	73.025	6	107.293	6 (Bilaterally)	0.0348	6 (Bilaterally)
S5-4Z2D	84.257	5	138.33	5 (Intact)	0.0318	5 (Defected)
S6-6Z	79.365	6	134.51	6 (Intact)	0.0287	6 (Defected)
S7-6Z	79.302	6	135.02	6 (Intact)	0.0291	6 (Defected)
S8-6Z	73.039	6	107.347	6 (Intact)	0.0328	6 (Defected)

V: Value **L**: Location

were seen in the ZIs placed at the location of the second premolar in the models S1, S3, and S5, while the stress values were seen in the ZIs, placed at the location of the first molar, in the models S2, S4, S6, S7, and S8 (Table 3) (Fig. 4).

The maximum bone deformation was seen in model S4 as 0.0348 mm and this value was followed by S8 with 0.0328 mm, S5 with 0.0318 mm, S3 with 0.0302 mm, S7 with 0.0291 mm, S6 with 0.0287 mm, S1 with 0.0175 mm and S2 with 0.0088 mm. The lowest bone deformation value was seen in model S2. The displacement values were ranked as S4 > S8 > S5 > S3 > S7 > S6 > S1 > S2. In the models S1, S2, S3, and S5, the maximum displacement value was at the location of the second premolar. In models S4, S6, S7, and S8, the maximum displacement value was at the location of the first molar (Table 3).

Discussion

In the literature, the success rate of ZIs has been reported between 94% and 100%.[18] Therefore, ZI is considered as an alternative treatment for resorbed or defective maxilla. Multiple ZI application can be an alternative treatment for situations that cannot be supported with DIs in the anterior defective premaxilla [12].

Several studies [19, 20] demonstrated predictable results as a result of using 2 ZIs with anterior DIs. Favorable clinical findings were reported also with quad zygomatic implants in the literature. It has been reported that cases in which 40 N torque was received during zygomatic implant are suitable for immediate loading [21]. The compact structure of the zygomatic bone allows immediate loading of the ZI. However, since zygomatic implants are applied in an angled position, horizontal forces are released during function, and this is biomechanically critical for implant success. Zygomatic implants can cause many complications in the implants or surrounding tissues. These include mechanical failure (in implants) and orbital damage maxillary sinusitis, soft tissue infection, paresthesia and fistula formation (in biological tissues) [22]. In addition, it has been reported that it provides the patient with a satisfactory function in a shorter time by avoiding invasive and extensive protocols [23].

To our knowledge, this is the first study to compare the biomechanics of rehabilitation approaches using six ZIs and four ZI combined with two DIs. As a result of the present study, the maximum Von Mises stress value was found in the maxilla model with a unilateral posterior defect, which was planned with four ZIs and two DIs. The present result indicates that the amount of stress will increase if the defect is asymmetric on the maxilla. The stress values in the S6 and S7 models, which were planned with six implants, are very close to each other, and these stress values were significantly higher than the other models planned with six implants. This result can be explained by the asymmetry of the defect, which creates a non-uniform force distribution on the prosthesis and creates a bending moment on the implants. On the defective side, a cortical layer of the maxilla is resected or was considerably decreased due to the resection. Therefore, the maximum stress value in the defected site was distributed into the trabecular bone in the defected area and could not be concentrated in the cortical layer. As a result of this, the maximum stress value was found on the cortical layer of the intact maxilla models, which seems contrary to expectations. Many biomechanical studies in the literature have reported that stress is concentrated in the cortical plate of the implant neck [24, 25]. The results reported in the present study can be explained by the above-mentioned mechanism.

Between all the same defect type models, the maximum Von Mises stress levels in the models with six ZIs were lower than the models with four ZIs combined with two DIs models. This result shows that additional zygomatic implants would provide higher biomechanical support than DIs in four zygoma implant rehabilitation, regardless of defect type. Akay et al. [17] evaluated three different implant-retained obturator prostheses in three models: model 1 with one ZI and one DI, model 2 with one ZI and two DIs, and model 3 with two ZIs.

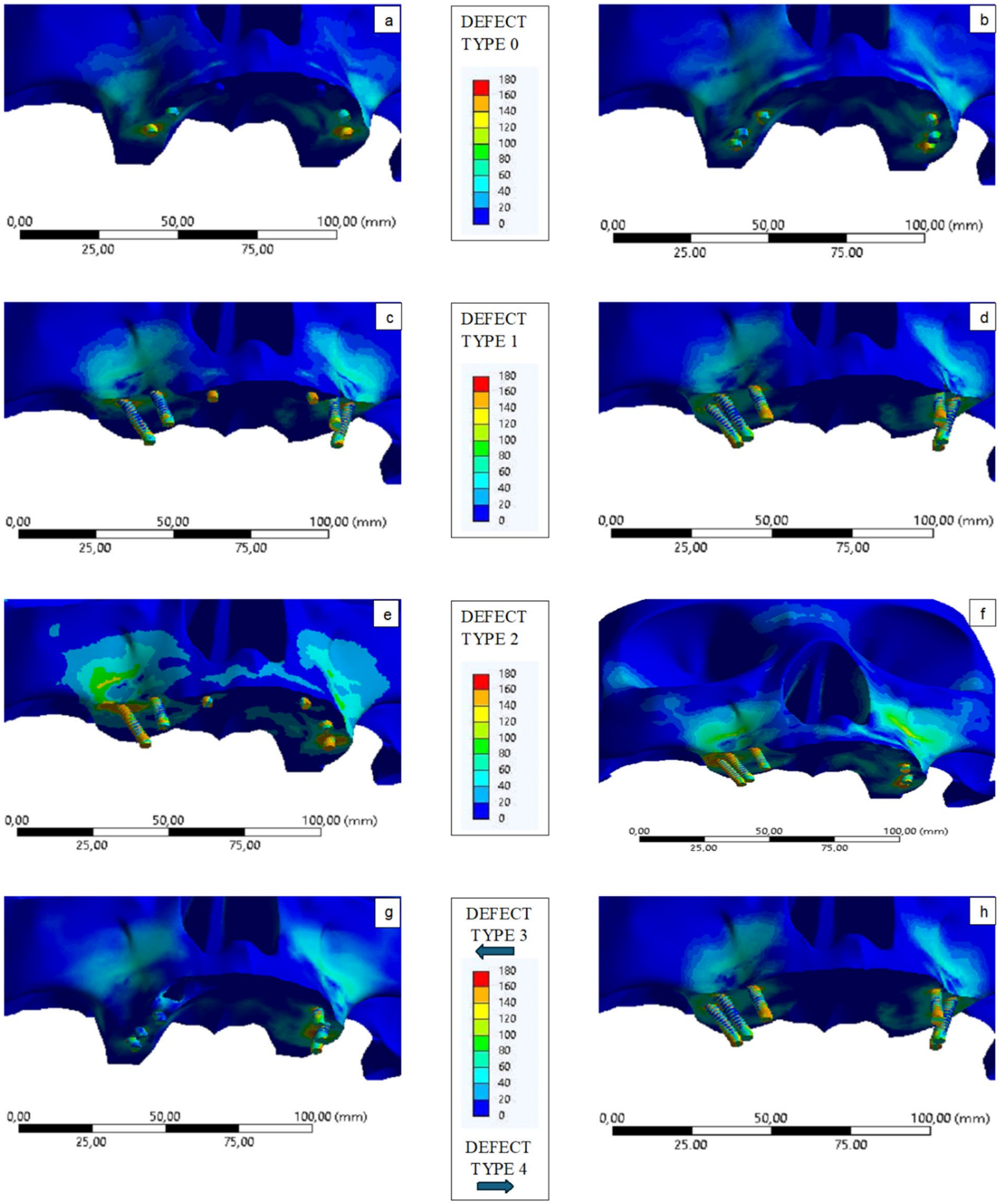

Fig. 3 Maximum Von Mises stress distribution on bone for each scenario. **a**: Scenario 1, **b**: Scenario 2, **c**: Scenario 3, **d**: Scenario 4, **e**: Scenario 5, **f**: Scenario 6, **g**: Scenario 7, **h**: Scenario 8

These authors reported that using two ZIs on each side of the maxilla is advantageous compared to the placement of DIs. In various studies on this subject, it has been reported that the use of ZIs generally reduces the amount of stress in the area without defect, and increasing the number of DIs reduces the stress distribution to a lesser extent [26, 27]. As a result of the current study, it is seen that the stress values obtained after the application

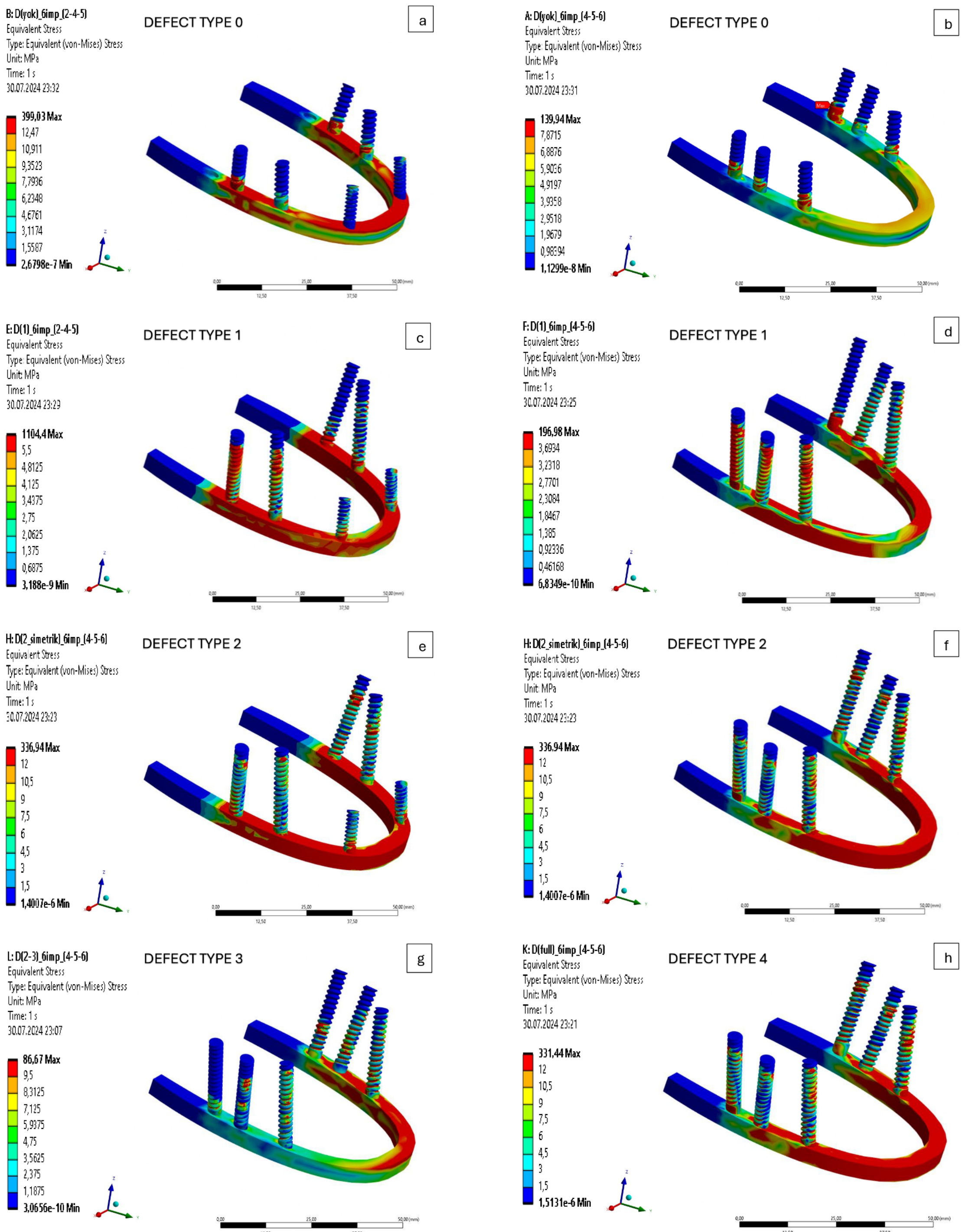

Fig. 4 Maximum Von Mises stress distribution in implants for each scenario **a**: Scenario 1, **b**: Scenario 2, **c**: Scenario 3, **d**: Scenario 4, **e**: Scenario 5, **f**: Scenario 6, **g**: Scenario 7, **h**: Scenario 8

of 6 ZIs are less than the stress values obtained after the application of DIs with 4 ZIs and this data is consistent with the studies cited above.

Among all implants, the highest maximum Von Mises stress level was found as 138.33 MPa in the scenario 5 model. Considering that the implant can tolerate up to 900 N/M^2 resistance without irreversible deformation in short term follow-up, it can be concluded that none of the eight scenarios tested in the present study are expected to cause irreversible damage to the implants [28].

In the present study, the maximum Von Mises stress values, seen in the bone around the ZIs, were found to be higher than the stress found in DIs; even the amount of stress per DI was negligible. This result is in line with the literature [29]. This result can be explained by the fact that due to the angled placement of ZIs, horizontal force occurs during function, in short, unlike the DI, the ZI is exposed to bidirectional force.

The highest stress values in the bone and implant were found in the most distal implant sites. In several studies, the maximal von Mises stress values were reported to be located around the distal implant neck regions in both cortical and cancellous bone, similar to the present study [30, 31]. This result can be explained by the application of force on the first premolar, second premolar, and first molar teeth, which is closer to the posterior implant, and with the same logic, the fact that the masseteric force is closer to the posterior implant. In a study comparing muscle activities in patients with dentate and ZI-supported prostheses in the literature, when the electromyography (EMG) values obtained were interpreted, a significant increase in masseter activity was found in patients who underwent ZI compared to patients with dentate prostheses [32]. This result can be explained by the sensation of stimulation caused by the presence of implants and denture base, despite the absence of periodontal nerve stimulation. In the current study, the high-stress value, especially in the posterior ZI, can be attributed to this activation in the masseter muscle and the effect of this activation on the surrounding implant.

The gold standard for evaluating stress distributed on the bone is the maximum principal stress, as well as the von Mises stress. Maximum principal stresses are components of stresses that occur when the basis of other stress tensors is zero and describe the stress concentrated in a particular region. Von Mises stress is a scalar quantity. It helps us to evaluate the yielding (or failure) of a ductile material. Bone is considered to be a semi-brittle material capable of exhibiting plasticity and ductility when conditions allow. Bone fracture differently under slow and rapid loading, becoming ductile and brittle, respectively. In the literature, while Maximum Principle Stress is used in some studies to evaluate the distribution of intra-bone stresses, Von Mises value is used in others. Since bone has a ductile structure and it is possible to distribute the acting forces to the surrounding tissues, it was deemed appropriate to use von Mises stress in this study [33, 34].

One of the limitations of this study is that the model was derived by scanning a solid model that mimics the anatomical dimensions of the skull exactly. The study can be developed using CT data obtained from several different sample patient groups. Although the material properties of the modeled structures are assigned individually, heterogeneous structural properties can be observed in living tissue. Since previous studies [15, 35] simulated the effect of the masseter muscle on the zygomatic bone, to improve the accuracy of the study results, the effect of the masseter muscle was simulated on the skull models in this study too. Although it is not possible in a virtual environment to perfectly reflect all the forces affected during real function, this study provides approximate results in biomechanical terms and offers the opportunity to compare between models.

Conclusion

The following conclusions can be drawn as the results of the present study:

1. The presence of alveolar defects affects the amount of stress in the bone and implant
2. With asymmetrical defects, the amount of stress on the prosthesis will be unevenly distributed, so that stress is increased relative to symmetrical defects;
3. When treating maxilla with defects, six maxillary ZI approaches will outperform (biomechanically) ZI plus DI approaches;

This study presents pilot data on ZI planning in the maxilla with an alveolar defect. In future work, it will be necessary to support these data with clinical trials.loading.

Abbreviations

FEA	Finite element analysis
3D	3-Dimensional
ZI	Zygomatic Implant
DI	Dental Implant

Acknowledgements

This study has been supported by the Recep Tayyip Erdoğan University Development Foundation, Grant Number: 02024007011009. We thank to Dr Muhammet Akın for his help with photo editing.

Author contributions

Z.G: Planning the methodology, analysis, interptetation of the results and writing. E.B: Interptetation of the results. Z.B: Interptetation of the results.

Funding

None.

Data availability

No datasets were generated or analysed during the current study.

Declarations

Ethics approval and consent to participate

Not applicable.

Consent for publication

Not applicable.

Competing interests

The authors declare no competing interests.

Received: 20 June 2024 / Accepted: 8 October 2024
Published online: 16 October 2024

References

1. Seerig LM, Nascimento GG, Peres MA, Horta BL, Demarco FF. Tooth loss in adults and income: systematic review and meta-analysis. J Dent. 2015;43(9):1051–9.
2. Pellegrino G, Tarsitano G, Basile F, Pizzigallo A, Marchetti C. Computer-Aided rehabilitation of maxillary oncological defects using zygomatic implants: a defect-based classification. J Oral Maxillofac Surg. 2015;73:e1-2446 e11.
3. Odman J, Lekholm U, Jemt T, Branemark PI, Thilander B. Osseointegrated titanium implants–a new approach in orthodontic treatment. Eur J Orthodont. 1988;10:98–105.
4. Wang F, Monje A, Lin GH, Wu Y, Monje F, Wang HL, Davo R. Reliability of four zygomatic implant-supported prostheses for the rehabilitation of the atrophic maxilla: a systematic review. Int J Oral Maxillofac Imp. 2015;30:293–8.
5. Duarte LR, Filho HN, Francischone CE, Peredo LG, Branemark PI. The establishment of a protocol for the total rehabilitation of atrophic maxillae employing four zygomatic fixtures in an immediate loading system–a 30-month clinical and radiographic follow-up. Clin Imp Dent Relat Res. 2007;9:186–96.
6. Padovan LE, Ribeiro-Junior PD, de Mattias Sartori IA, Thome G, Sartori EM, Uhlendorf J. Multiple zygomatic implants as an alternative for rehabilitation of the extremely atrophic maxilla: a case letter with 55 months of follow-up. J Oral Implantol. 2015;41:97–100.
7. Branemark PI. Surgery and fixture installation: zygomaticus fixture clinical procedures. Gothenburg, Sweden, Nobel Biocare AB; 1998, p. 1.
8. Aparicio CMC, Francisco K, Claros P, Alandez J, Gonzalez-Martin O, Albrektsson T. Zygomatic implants: indications, techniques and outcomes, and the zygomatic success code. Periodontol. 2014;2000 66:41–58.
9. Duan Y, Chandran R, Cherry D. Influence of alveolar bone defects on the stress distribution in Quad Zygomatic Implant-supported Maxillary Prosthesis. Int J Oral Maxillofac Imp. 2018;33:693–700.
10. Davo R, Pons O, Rojas J, Carpio E. Immediate function of four zygomatic implants: a 1-year report of a prospective study. Eur J Oral Implantol. 2010;3:323–34.
11. Padovan LEV, Ribeiro-Júnior PD, de Mattias Sartori IA, Thomé G, Sartori EM, Uhlendorf J. Multiple zygomatic implants as an Alternative for Rehabilitation of the extremely atrophic Maxilla: a Case Letter with 55 months of Follow-Up. J Oral Implantol. February 2015;1(1):97–100.
12. Bothur S, Jonsson G, Sandahl L. Modified technique using multiple zygomatic implants in reconstruction of the atrophic maxilla: a technical note. Int J Oral Maxillofac Implants. 2003;18:902–4. Nov-2003.
13. Lekholm U, Zarb GA, Albrektsson T. Patient selection and preparation. Tissue integrated prostheses. Chicago: Quintessence Publishing Co. Inc. 11985:99–209.
14. Gümrükçü Z. Biomechanical evaluation of Zygomatic Implant Use in patients with different buccal Maxillary defect levels. Int J Oral Maxillofac Implants. 2019;34:e115–22.
15. Ishak MIAKM, Sulaiman E, Abu Kasim NH. Finite element analysis of different surgical approaches in various occlusal loading locations for zygomatic implant placement for the treatment of atrophic maxillae. Int J Oral Maxillofac Surg. 2012;41:1077–89.
16. Varghese KG, Kurian N, Gandhi N, Gandhi S, Daniel AY, Thomas HA, Sudharson NA, Wadhwa S. Three-dimensional finite element analysis of zygomatic implants for rehabilitation of patients with a severely atrophic maxilla. J Prosthet Dent. 2023;129(4):e5971–8.
17. Akay C, Yalug S. Biomechanical 3-dimensional finite element analysis of obturator protheses retained with zygomatic and dental implants in maxillary defects. Med Sci Monit. 2015;21:604–11.
18. Lorusso F, Conte R, Inchingolo F, Festa F, Scarano A. Survival rate of zygomatic implants for fixed oral Maxillary rehabilitations: a systematic review and Meta-analysis comparing outcomes between zygomatic and regular implants. Dentistry J. 2021;9(4):38.
19. Balshi TJ, Wolfinger GJ, Petropoulos VC. Quadruple zygomatic implant support for retreatment of resorbed iliac crest bone graft transplant. Implant Dent. 2003;12:47–53.
20. Kuabara MR, Ferreira EJ, Gulinelli JL, Panzarini SR. Use of 4 immediately loaded zygomatic fixtures for retreatment of atrophic edentulous maxilla after complications of maxillary reconstruction. J Craniofac Surg. 2010;21:803–5.
21. Esposito M, Grusovin MG, Achille H, Coulthard P, Worthington HV. Interventions for replacing missing teeth: different times for loading dental implants. Cochrane Database Syst Rev. 2009:CD003878.
22. Chrcanovic BR, Abreu MH. Survival and complications of zygomatic implants: a systematic review. Oral Maxillofac Surg. 2013;17:81–93.
23. Stievenart M, Malevez C. Rehabilitation of totally atrophied maxilla by means of four zygomatic implants and fixed prosthesis: a 6-40-month follow-up. Int J Oral Maxillofac Surg. 2010;39:358–63.
24. Chang SH, Lin CL, Hsue SS, Lin YS, Huang SR. (2012) Biomechanical analysis of the effects of implant diameter and bone quality in short implants placed in the atrophic posterior maxilla. Med Eng Phys.2012;34:153 – 60.
25. Demenko V, Linetsky I, Nesvit V, Linetska L, Shevchenko A. FE study of bone quality effect on load-carrying ability of dental implants. Comp Methods Biomech Biomed Eng. 2014;17:1751–61.
26. Chao YL, Meijer HJ, Van Oort RP, Versteegh PA. (1995) The incomprehensible success of the implant stabilised overdenture in the edentulous mandible: a literature review on transfer of chewing forces to bone surrounding implants. Eur J Prosthodont Restor Dent. 1995;3:255 – 61.
27. Meijer HJ, Starmans FJ, Steen WH, Bosman. A three-dimensional finite element study on two versus four implants in an edentulous mandible. Int J Prosthodont. 1994;7:271–9.
28. Zarone F, Apicella A, Nicolais L, Aversa R, Sorrentino R. Mandibular flexure and stress build-up in mandibular full-arch fixed prostheses supported by osseointegrated implants. Clin Oral Imp Res. 2003;14:103–14.
29. Wen H, Guo W, Liang R, Xiang L, Long G, Wang T, Deng M, Tian W. Finite element analysis of three zygomatic implant techniques for the severely atrophic edentulous maxilla. J Prosth Dent. 2014;111:203–15.
30. Barao VA, Delben JA, Lima J, Cabral T, Assuncao WG. Comparison of different designs of implant-retained overdentures and fixed full-arch implant-supported prosthesis on stress distribution in edentulous mandible–a computed tomography-based three-dimensional finite element analysis. J Biomech. 2013;46:1312–20.
31. Correa S, Ivancik J, Isaza JF, Naranjo M. Evaluation of the structural behavior of three and four implant-supported fixed prosthetic restorations by finite element analysis. J Prosthodont Res. 2012;56:110–9.
32. de Rossi M, Palinkas M, de Lima-Lucas B, Santos CM, Semprini M, Oliveira LF, Hallak-Regalo I, Bersani EO, Miglioranca R, Siéssere S, Hallak-Regalo SC. Masticatory muscle activity evaluation by electromyography in subjects with zygomatic implants. Med Oral Patol Oral Cir Bucal. 2017; 1;22(3):e392-e397.
33. Yemineni BC, Mahendra J, Nasina J, Mahendra L, Shivasubramanian L, Perika SB. Evaluation of maximum principal stress, Von Mises Stress, and deformation on surrounding mandibular bone during insertion of an Implant: A three-dimensional finite element study. Cureus. 2020;12(7):e9430.
34. Zioupos P, Kirchner HOK, Peterlik H. Ageing bone fractures: the case of a ductile to brittle transition that shifts with age. Bone. 2020;131:115176.
35. Ujigawa K, Kato Y, Kizu Y, Tonogi M, Yamane GY. Three-dimensional finite elemental analysis of zygomatic implants in craniofacial structures. Int J Oral Maxillofac Surg. 2007;36:620e625.

Publisher's note